N O T I C E

THIS DOCUMENT HAS BEEN REPRODUCED FROM MICROFICHE. ALTHOUGH IT IS RECOGNIZED THAT CERTAIN PORTIONS ARE ILLEGIBLE, IT IS BEING RELEASED IN THE INTEREST OF MAKING AVAILABLE AS MUCH INFORMATION AS POSSIBLE

NASA Contractor Report 165600

DESIGN OF SUPERCRITICAL CASCADES WITH HIGH SOLIDITY

Jose M. Sanz
Universities Space Research Association
Columbia, Maryland 21044

February 1982

Prepared for
NATIONAL AERONAUTICS AND SPACE ADMINISTRATION
Lewis Research Center
Under Contract NAS3-2253

DESIGN OF SUPERCRITICAL CASCADES WITH HIGH SOLIDITY

Jose M. Sanz*
Universities Space Research Association
Columbia, Maryland 21044

Abstract

The method of complex characteristics of Garabedian and Korn has been successfully used to design shockless cascades with solidities of up to one. A new code has been developed using this method and a new hodograph transformation of the flow onto an ellipse. This new code allows the design of cascades with solidities of up to two and larger turning angles. The equations of potential flow are solved in a complex hodograph-like domain by setting a characteristic initial value problem and integrating along suitable paths. The topology that the new mapping introduces permits a simpler construction of these paths of integration.

1. Introduction

The design of supercritical blades for turbomachinery relies heavily on the capability of producing a wide variety of two-dimensional blade sections, spanning from hub to tip and varying from upstream to downstream stages. A code to design these sections will have to cover a broad spectrum of design flow conditions. It should be able to handle both low and high solidities, chord-to-gap ratios of up to two, as well as high incidence angles and Mach numbers.

The method of complex characteristics and hodograph transformation developed by Bauer, Garabedian and Korn, [1], to design supercritical wing sections and cascades has been widely used. With this method, excellent shockless airfoils have been designed and tested in this country and abroad. In its latest version, the method solves the problem of finding a shockless airfoil with a given pressure distribution.

Because of the conformal mapping used by Bauer, Garabedian and Korn to transform the hodograph domain of the flow onto a circle, a restriction exists in their method which does not allow the design of cascades with high solidities. Also, a poor resolution at the leading and trailing edge regions may arise, in cases of high incidence angles, as a consequence of this mapping.

In this paper a new design technique is described, based on the same complex characteristics method, which uses a new mapping of the hodograph domain onto an ellipse. This new mapping leads naturally to the use of Tchebicheff polynomials, rather than trigonometric polynomials, to construct the solution of the equations. The equations of flow are integrated along a new set of paths which are more in accord with the topology that the elliptic mapping introduces.

The heuristic idea behind the elliptic mapping is the following. When the flow is mapped onto a circle, the upstream and downstream points of infinity are mapped into two interior points of the circle, where two logarithmic singularities of the solution, a source and a sink, are located. By increasing the separation between these two points the gap-to-chord ratio can be reduced. The limiting case of infinite gap-to-chord ratio, or the isolated airfoil, corresponds to the case in which both singularities coalesce. By mapping the flow onto an ellipse, the two singularities can be more widely separated, further reducing the gap-to-chord ratio. A parameter related to the eccentricity of the ellipse will be introduced to control the solidity of the cascade.

With this new method we have achieved high solidities. A good resolution of points defining the body is obtained both at the leading and trailing edge regions and larger incidence angles, with thinner airfoils, can be achieved. In the next section we review the method of complex characteristics, as applied to our problem.

Professor Paul R. Garabedian of the Courant Institute of Mathematical Sciences proposed this problem and made many suggestions during the development of the code.

2. Hodograph Complex Equations

The equations of potential flow in hodograph coordinates can be described by the Chaplygin system

$$\varphi_q = \frac{M^2 - 1}{\rho q}\psi_\theta$$
$$\varphi_\theta = \frac{q}{\rho}\psi_q, \qquad (1)$$

in which φ and ψ are the potential, and stream functions, M is the local Mach number, q and θ are respectively the modulus and argument of the velocity vector, and ρ is the density. This system of equations is of mixed type, elliptic and hyperbolic, in the transonic regime.

In the method of complex characteristics, the variables are analytically extended into the four dimensional domain of two complex variables, where the characteristic equations can always be solved. The system (1) can be written in the canonical form, [1],

$$\varphi_\xi = \tau_+\psi_\xi$$
$$\tau_\pm = \pm i\,\frac{\sqrt{1 - M^2}}{\rho}, \qquad (2)$$
$$\varphi_\eta = \tau_-\psi_\eta$$

The two independent variables ξ and η are arbitrary complex analytic functions of the characteristic coordinates

*Visiting Research Scientist presently at NASA Lewis Research Center, Fluid Mechanics and Acoustics Division, Computational Fluid Mechanics Branch, Cleveland, Ohio 44135.

$$s = \log h - i\theta$$
$$t = \log h + i\theta, \tag{3}$$

where h is defined by

$$h(q) = h(C_*)\, e^{\int_{C_*}^{q} \sqrt{1 - M^2}/q'\ dq'},$$

$$h(C_*) = e^{\int_{1}^{C_*} \sqrt{1 - M^2}/q'\ dq'} \tag{4}$$

and C_* is the critical speed.

We recall that the coordinates s and t are conjugated characteristics coordinates, [1], in the subsonic domain. This means that, for subsonic points, s and t are complex conjugate numbers when q and θ are real. If the variables ξ and η are defined in the form

$$s = f(\xi),\ t = \overline{f(\overline{\eta})}, \tag{5}$$

with f analytic, then they are also conjugate coordinates. Under this transformation the sonic surface is mapped onto a curve of each characteristic plane, called the sonic locus, [1].

In the hodograph method, we are interested in solving an inverse problem. We construct a solution with the correct logarithmic singularities, which represent a sink and source at infinity, and we look at the zero stream line, on the phisical real plane, as the possible candidate for the body which generates the flow.

In the context of the complex system (2), the correct mathematical problem to solve is the characteristic initial value problem where initial data is given in the two characteristic planes emanating from the initial point (ξ_0, η_0) in the four-dimensional space. The manipulation of this initial data can and has lead in the past, [1], to the construction of shockless solutions. A new and fundamental approach in the application of hodograph methods was taken in [2], where the unknown domain of the flow is mapped onto the unit circle, by a conformal mapping of the type (5). This allows for a systematic prescription of the initial characteristic data, based on a given pressure distribution over the airfoil. In the next section we describe how this idea is implemented.

3. Elliptic Conformal Transformation

Following the idea described in the last paragraph, we use the transformation (5) to map the flow onto an elliptic domain D of each coordinate characteristic plane. Because of this transformation, the coordinate characteristics are such that real subsonic points correspond to the domain of points of the form $(\xi, \bar{\xi})$, when ξ is a point enclosed by the portion of the boundary of D where ξ and η are conjugate coordinates and the sonic locus. This part of the boundary will correspond to the subsonic part of the body. Points in the remainder of the domain D do not correspond to the real physical plane, and the real supersonic part of the body have to be found by searching for the zero stream line.

The elliptic domain and the corresponding Tchebycheff polynomials can be defined in the following form. Consider the conformal mapping

$$\omega = \frac{1}{2}\left(\xi + \frac{1}{\xi}\right),\ 1 \le |\xi| \le R \tag{6}$$

of a circular ring in the plane onto the ellipse with axes defined by the points

$$\pm \frac{1}{2}\left(R + \frac{1}{R}\right),\ \pm \frac{1}{2}\left(R - \frac{1}{R}\right)$$

and the slit $(-1,1)$. We consider the class of analytic functions in the ring which have a Laurent expansion of the form

$$F(\xi) = \sum_{-\infty}^{\infty} a_n \xi^n = \sum_{0}^{\infty} a_n \left(\xi^n + \frac{1}{\xi^n}\right), \tag{7}$$

in which $a_n = a_{-n}$, for all positive n. The functions of the variable ω

$$T_n(\omega) = \frac{1}{2^n}\left(\xi^n + \frac{1}{\xi^n}\right),\ n = 0, 1, 2, \ldots \tag{8}$$

are actually the Tchebycheff polynomials of the first kind, as can be easily verified.

We observe that a function of the type (7) has the property

$$F(e^{i\theta}) = F(e^{-i\theta}),\ 0 \le \theta \le \pi \tag{9}$$

This means that within this class of functions, we are identifying points with the same real part in the positive and negative parts of the unit circumference. Any analytic function on the ellipse in the ω-plane can then be written in the form

$$F(\omega) = \sum_{0}^{\infty} a_n \left(\xi^n + \frac{1}{\xi^n}\right)$$

$$= \sum_{0}^{\infty} a_n' T_n(\omega) = \sum_{0}^{\infty} b_n \omega^n \tag{10}$$

This shows that the ellipse is equivalent to the circular ring with the given identification of points on the unit circumference. This identification actually makes unnecessary the slit introduced by the mapping (6), making the elliptic domain singly connected.

We adopt as our computational domain, D, the circular ring $1 \le |\xi| \le R$, with the previous identification of points. The parameter R will control the eccentricity of the ellipse and, in this way, the solidity of the cascade. Several advantages arise from this formulation. The most

important one is that we are now able to use Fast Fourier Transform to compute the coefficients of the mapping function

$$f(\xi) = \sum_{0}^{\infty} a_n \left(\xi^n + \frac{1}{\xi^n}\right) \tag{11}$$

of the flow onto our computational domain D. Other advantages of this formulation will be discussed later.

The supercritical design problem can be formulated as follows. Find an analytic solution

$$\varphi(\xi,\eta) = R_e\{\varphi_1(\xi,\eta) \log(\eta - \eta_1) + \varphi_2(\xi,\eta) \log(\eta - \eta_2) + \varphi_3(\xi,\eta)\}$$

$$\psi(\xi,\eta) = R_e\{\psi_1(\xi,\eta) \log(\eta - \eta_1) + \psi_2(\xi,\eta) \log(\eta - \eta_2) + \psi_3(\xi,\eta)\} \tag{12}$$

of the system (2), with $\varphi_1,\varphi_2,\varphi_3$ and ψ_1,ψ_2,ψ_3 regular functions, in the domain D, where the mapping function f defined by (11), satisfies the Dirichlet condition

$$R_e(f(\xi)) = \log(h^*(q)), \quad |\xi| = R, \tag{13}$$

and the stream function satisfies the boundary condition

$$R_e(\psi(\xi,\bar{\xi})) = 0, \quad |\xi| = R. \tag{14}$$

The stream function is real valued for subsonic points and the boundary condition (14) is well defined when a proper branch of the solution is taken. The function h^* is defined by

$$h^*(q) = h(C_*)\, e^{k\left|\int_{C_*}^{q} \sqrt{1-M^2}\, dq'/q'\right|}, \quad k > 0. \tag{15}$$

The regular part of the solution, can be expanded as a linear combination of particular solutions obtained by taking as initial characteristic data a complete set of ortonormal functions, namely the Tchebycheff polynomials. The coefficients of this linear combination are then determined by imposing the boundary condition (14). This boundary value problem has been proved to be well posed when the system (1) is reduced to Tricomi equation, [4], that is, in the case of the transonic small disturbance equation. In the general case of the full potential equation that we are dealing with here, a low condition number for the matrix associated with the linear system in question, both when the domain D is a circle or an ellipse, indicates the well posedness of the problem.

With the definitions given, h^* and h become identical in the subsonic part of the domain D, where we take the parameter k equal to unity. In the remainder of this domain, h is not real and the introduction of the function h^* becomes necessary. The consequence of using this Dirichlet condition is that the designed airfoil will not achieve the prescribed pressure distribution on the supersonic part of the airfoil.

The boundary conditions (13) and (14) are nonlinearly coupled. The nonlinearity of the problem arises from the fact that the speed distribution is given as a function of the arc length, and in (13) it is needed as a function of the coordinate ξ on the boundary $|\xi| = R$. The relationship between ξ and the arc length s, can only be determined when the potential function is known. On the other hand, the solution of the boundary value problem (14) is linked to the knowledge of the mapping function f. An iterative procedure is then needed to solve the problem.

This iterative procedure is established by first computing an incompressible solution $\varphi(\xi),\psi(\xi)$ on the elliptic domain, in terms of classic Jacobi elliptic functions. The incompressible solution is conformal invariant. We can then, establish the relation between the arc length s and the boundary variable $\xi = Re^{i\theta}$, as we know $\varphi(s)$. This allows computation of the mapping function f, using F.F.T. to solve the Dirichlet problem (13) with prescribed values of h^* at a number N of equidistant nodes on the circumference of radius R.

Once the mapping function is known, the system (2) can be integrated, as $\tau_\pm$ are, then, known functions of the variables ξ and η. We remark that at each iteration an analytic solution is found. If the zero stream line is not self intersecting and has the proper closure at the trailing edge, it represents a shockless airfoil.

4. Numerical Solution

We concentrate in this section in the problem of finding a solution of the type (12) to the system (2), once the mapping function f has been determined. We introduce the notation

$$L_\xi(\varphi,\psi) = \varphi_\xi - \tau_+\psi_\xi$$

$$L_\eta(\varphi,\psi) = \varphi_\eta - \tau_-\psi_\eta$$

The requirement that the functions (12) are solutions of the system (2) with the pairs $(\varphi_i,\psi_i)\, i = 1,3$ being regular functions leads to the homogeneous system, for each value $i = 1,2$ of the index i,

$$L_\xi(\varphi_i,\psi_i) = 0$$

$$L_\eta(\varphi_i,\psi_i) = 0 \tag{16}$$

with

$$\varphi_i = \tau_+\psi_i \quad \text{on} \quad \eta = \eta_i, \; i = 1,2 \tag{17}$$

and to the inhomogeneous system

$$L_\xi(\varphi_3,\psi_3) = 0$$

$$L_\eta(\varphi_3,\psi_3) = -\left(\sum_{i=1}^{2} \frac{\varphi_i - \tau_+\psi_i}{\eta - \eta_i}\right). \tag{18}$$

The problem (16) with the condition (17) is known as the Riemann problem for that system. The solutions are the Riemann functions related to that problem and can be explicity integrated along the characterstic $\eta = \eta_i$, in the form

$$\psi_i(\xi,\eta_i) = \frac{C_i}{\sqrt{\tau_+(\xi,\eta_i)}}$$

$$\varphi_i(\xi,\eta_i) = C_i \sqrt{\tau_+(\xi,\eta_i)} \tag{19}$$

and $i = 1,2$.

The complex constants C_1 and C_2 remain at our disposal. These two sets of Riemann functions can be integrated with a finite difference scheme, that will be described later. We can impose on the $\xi = \xi_i$, $i = 1,2$, characteristics the initial data

$$\psi_i(\xi_i,\eta) = \overline{\psi_i(\bar{\eta},\bar{\xi}_i)}$$

$$\varphi_i(\xi_i,\eta) = \overline{\varphi_i(\bar{\eta},\bar{\xi}_i)}. \tag{20}$$

Once these functions are determined, we can integrate the inhomogeneous system (18). For that, we expand the solution in the form

$$\varphi_3 = \varphi_3^{(o)} + \sum_1^N b_n\varphi_3^{(n)}$$

$$\psi_3 = \psi_3^{(o)} + \sum_1^N b_n\psi_3^{(n)} \tag{21}$$

where $(\varphi_3^{(o)},\psi_3^{(o)})$ is a solution of the inhomogeneous problem (18) with the homogenous initial characteristic data

$$\psi_3^{(o)}(\xi,\eta_3) = \overline{\psi_3^{(o)}(\bar{\eta}_3,\bar{\xi})} = 0, \tag{22}$$

assigned on the two characteristics emanating from a point $(\xi_3,\bar{\xi}_3)$, which is subsonic and far from the singularities $(\xi_1,\bar{\xi}_1)$ and $(\xi_2,\bar{\xi}_2)$. Each pair of functions $(\varphi_3^{(n)},\psi_3^{(n)})$ are solutions of the homogeneous system (16), with the initial characteristic data

$$\psi_3^{(n)}(\xi,\eta_3) = \overline{\psi_3^{(n)}(\bar{\eta}_3,\bar{\xi})} = T_n(\omega), \quad n = 1, \ldots, N \tag{23}$$

and where the $T_n(\omega)$ are the Tchebicheff polynomials described in (8). Once each of these initial characteristic problems is numerically solved, the coefficients b_n on (21) can be determined by imposing the boundary condition (14).

A rectangular grid is used to numerically solve each initial characteristic problem. Two sides of this rectangular grid are formed by two paths of integration, one in each characteristic plane. These paths allow one to reach the desired part of the flow to be computed. Three kinds of paths of integration are used, subsonic, transonic and supersonic paths.

To reduce the amount of computation, we divide the exterior circumference into eight sectors and we always take as initial point $(\xi_3,\bar{\xi}_3)$ the identical points $(0,1)$ and $(0,-1)$. From each singularity $(\xi_1,\bar{\xi}_1)$ and $(\xi_2,\bar{\xi}_2)$ we lay a path which goes directly to the point $(\xi_3,\bar{\xi}_3)$ to compute the Riemann solutions. The corresponding η-path will be the complex conjugate of the ξ-path. Once we reach the characteristics through the point $(\xi_3,\bar{\xi}_3)$ we continue computing the Riemann solutions plus the solution of the inhomogeneous problem (18) in the way described.

In those sectors in which all the nodes are subsonic points, we use subsonic paths. In this case the η-path is the complex conjugate of ξ-path. As ξ and η are conjugate coordinates at subsonic points, the diagonal of the rectangle corresponds to real subsonic points. The initial data has previously been defined by the reflection laws (20), (22), and (23). In this form the computation can be reduced to the triangle below the diagonal. A path will consist, then, of a segment that starts at ξ_3, ends at the outer circle, and continues with the circular arc corresponding to the sector in question.

In those sectors, below the sonic locus, where all, or some, of the nodes do not correspond to real subsonic points we use transonic paths. The idea is that to reach those points beyond the sonic line, the two-dimensional manifold formed by the two paths has to avoid the sonic surface $M(\xi,\eta) = 1$, where the equations become ill conditioned. So, in the case of those paths, we want the ξ-path and the η-path to not be conjugates of each other. The idea is, as in [1], to traverse the corresponding sector in opposite directions for each path.

Finally, the supersonic paths compute the real supersonic zone of the body. They were introduced first by Swenson and they use the property that a point in the real supersonic zone can be reached by two characteristics starting at the sonic locus of each characteristic plane, [1], [5]. The computation for the supersonic zone is done once the coefficients b_n in (21) have been obtained. So the problem (18) is solved only once for these points. This makes affordable, both in terms of computing storage and C.P.U. time, the use of a much finer grid for the supersonic computation. The analytic solution is path independent, by the Cauchy Integral theorem, provided that we stay on the proper branch of the solution.

The finite difference scheme

$$\psi_{i,j} - \psi_{i-1,j} = \tilde{\tau}_+(\psi_{i,j} - \psi_{i-1,j})$$

$$\psi_{i,j} - \psi_{i,j-1} = \tilde{\tau}_-(\psi_{i,j} - \psi_{i,j-1}) \qquad (24)$$

is used to integrate the equations. The average values $\tilde{\tau}_\pm$ are calculated with a predictor-corrector scheme which gives second-order accuracy. A Richardson extrapolation to the zero limit included in the code gives third-order accuracy.

Two complex constants were left at our disposal in the computation of the Riemann functions. To determine them we require, first, the stream function to be single valued along the airfoil. This leads to the condition for the jump in ψ

$$[\psi] = -2\pi\left[I_m\{\psi_1(\xi_1,\bar{\xi}_1)\} + I_m\{\psi_2(\xi_2,\bar{\xi}_2)\}\right] = 0 \qquad (25)$$

On the other hand, the circulation Γ over the airfoil is given. This imposes the jump condition on φ

$$I_m\{\varphi_1(\xi_1,\bar{\xi}_1)\} - I_m\{\varphi_2(\xi_2,\bar{\xi}_2)\} = \frac{\Gamma}{2\pi} \qquad (26)$$

The location of the stagnation point and trailing edge impose the two remaining conditions needed to determine the four real constants.

With the potential and stream functions completely determined, the body is calculated using the formula

$$x + iy = \int \frac{e^{i\theta}}{q}\left(d\varphi + \frac{i}{\rho}\, d\psi\right) \qquad (27)$$

By looking at the residuum of this function, when a loop is described around one singularity, say the source $\xi = \xi_2$, we obtain the repeating vector

$$[x + iy] = -2\pi \frac{e^{i\theta_2}}{q_2}$$

$$\times\left[I_m\{\varphi_2(\xi_2,\bar{\xi}_2)\} + \frac{i}{\rho_2} I_m\{\psi_2(\xi_2,\bar{\xi}_2)\}\right]. \qquad (28)$$

The modulus of this vector is the gap, or distance between adjacent blades. If we consider, instead, a loop which contains both singularities, we obtain the jump in the function $x + iy$ around the airfoil

$$[x + iy] = -2\pi$$

$$\times\left[\sum_{j=1}^{2} \frac{e^{i\theta_j}}{q_j}\left(I_m\{\varphi_j(\xi_j,\bar{\xi}_j)\} + \frac{i}{\rho_j} I_m\{\psi_j(\xi_j,\bar{\xi}_j)\}\right)\right] \qquad (29)$$

The real and imaginary parts of this vector measures the opening of the airfoil at the trailing edge in the x and y-directions, respectively. This formula can be used to check the accuracy of the computation, when the actual coordinates of the body are obtained.

5. Results

A computer code has been written to implement the method described. The purpose of the code is to extend the possibilities of the Bauer-Garabedian-Korn design code. We have followed, when possible, their method. A different strategy is used in the numerical solution of the equations, because of the different domain into which the flow is mapped.

The code uses as input a given speed distribution. Other parameters used include the following: the external radius R of the circular ring, which controls the solidity, the number of nodes in the exterior circle, equal to the number of Tchebycheff polynomials used in the expansion of the regular part of the solution, the number of iterations, which controls the total number of cycles (each one includes the calculation of the mapping function and a complete solution of the equations). Additionally, two grid sizes can be set, one for the subsonic-transonic computation, and the other, a finer one, for the supersonic computation. A Richardson extrapolation can be included in the last iteration. The inlet Mach number is specified in the case of compressor design, and the exit Mach number is specified in the case of turbines.

A typical run takes 12 minutes of IBM 370-3033 CPU time. We remark that, while a blade design can imply many runs to achieve the desired design conditions, most of these runs can be executed with a coarse grid, small number of nodes, and only one iteration, which can reduce the C.P.U. time of each run to less than one minute, until the approximate design conditions are obtained.

Figure 1 represents a high solidity cascade designed with the new code. A solidity of 2.05 was obtained, with a turning angle of 42 degrees. The supersonic zone reached, though, has a moderate peak Mach number of 1.07. We use 128 nodes which delivers 193 computed points on the body. It can be seen that a good resolution of points is obtained both at the leading and trailing edge. Figure 2 represents a typical hodograph plane with the integration paths. Figure 3 shows a highly staggered rotor tip section with an inlet flow angle of 55 degrees.

6. Conclusions

A new design method has been developed for the design of supercritical cascades based on an elliptic conformal transformation of the hodograph plane and the use of complex characteristics. With this new method we have been able to handle high solidity cascades.

Because we use, as in the Bauer-Garabedian-Korn method, an input pressure distribution the code can easily be coupled with a boundary layer calculation. In this way, the pressure distribution can be modified until the desired separation criteria is met.

The effects of the stream tube convergence and radius change in the design of turbomachinery blades are well known. The incorporation of those effects in the present code would enhance its capabilities. A possible way to achieve this would be by reducing the three-dimensional problem to a set of two-dimensional problems by means of a Garlekin-type decomposition. The presence of a shroud in turbomachinery rows makes this method more appealing than in the case of isolated airfoils.

7. References

1. Bauer, F., Garabedian, P. and Korn, D.: "Supercritical Wing Sections", Vol I, II, III, Springer-Verlag, 1972, 1975, 1977.
2. Garabedian, P. and Korn, D., "A Systematic Method for Computer Design of Supercritical Airfoils in Cascades", Comm. Pure and Appl. Math, Vol XXIX, 1976.
3. Korn, D., "Numerical Design of Transonic Cascades", Journal of Computational Physics, 29, 20-34, 1978.
4. Sanz, J., "A Well Posed Boundary Value Problem in Transonic Gas Dynamics", Comm. Pure and Appl. Math., Vol XXXI, 1978.
5. Swenson, E., "Geometry of the Complex Characteristics in Transonic Flows", Comm. Pure and Appl. Math., Vol XXI, 1968.
6. Garabedian, P. "Partial Differential Equations", Wiley, New York, 1962.

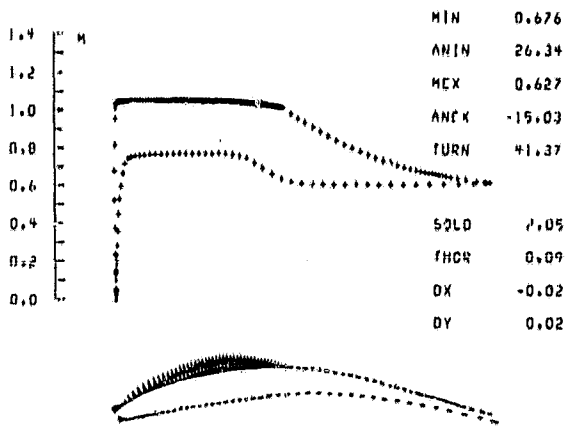

Fig 1. High solidity stator blade

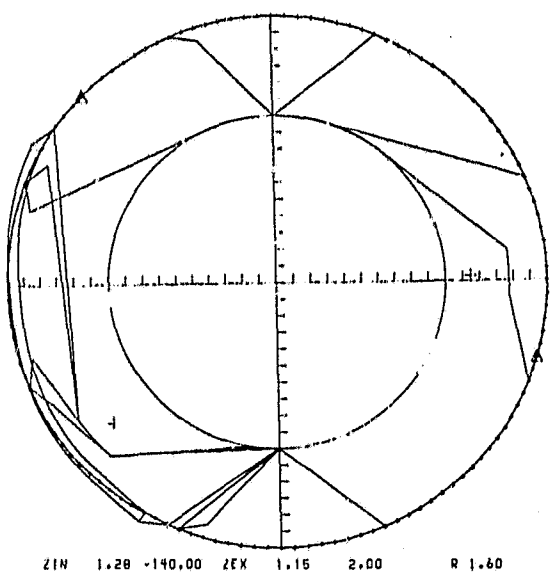

Fig 2. Hodograph plane

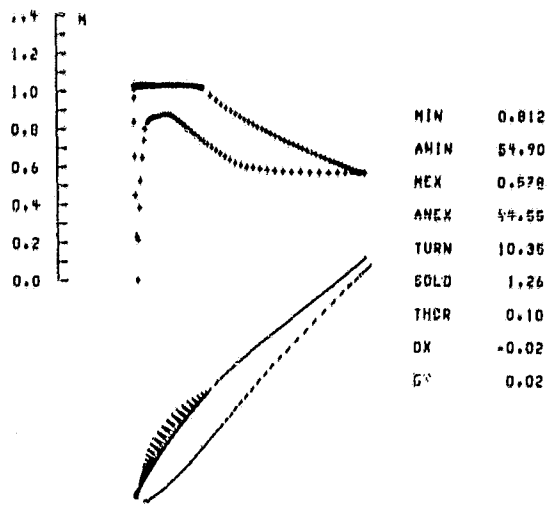

Fig 3. High stagger rotor blade